Materials Today: Proceedings 72 (2023) 3081–3088

Contents lists available at ScienceDirect

Materials Today: Proceedings

journal homepage: www.elsevier.com/locate/matpr

Comparative analysis of cross flow and jet impingement techniques of heat sink in electronics cooling

Deerajkumar Parthipan, Deepakkumar Rajagopal *

Department of Thermal and Energy Engineering, School of Mechancal Engineering, Vellore Institute of Technology, Vellore, India

ARTICLE INFO

Article history:
Available online 23 September 2022

Keywords:
Electronics cooling
Heat sink
Jet impingement
Cross flow
Computational fluid dynamics

ABSTRACT

New and advanced technologies lead to the miniaturization of electronic devices with high energy densities. Though this is commendable progress in electronic technology, cooling these systems has become arduous due to the high heat flux generation from these devices. Traditional cooling systems are lagging due to these challenges, which brings up the demand for novel cooling techniques for this purpose. This research paper focused on the comparison of cross flow and jet impingement cooling techniques used in the heat sink, the peak temperature raised and the pressure drop across the heat sink is reported. The computational Fluid Dynamics (CFD) technique is used to investigate the flow and heat transfer characteristics. Among the cases studied, it is identified that the cross-flow shows superior thermal attributes as compared to the jet impingement method, due to which the base temperatures of pin fins in the cross-flow is noticed an average of 14.5° C lower than that of jet impingement.

Selection and peer-review under responsibility of 2nd International Conference on Sustainable Materials, Manufacturing and Renewable Technologies 2022 (i-SMART 2022).

1. Introduction

The rapid development of electronic technology has led to the growth of micro and mini- scale electronic industry, resulting in very high-power densities, thus leading to high heat flux generation. Additionally, due to the increasing integration of devices (e.g., transistors), the chip's or device's power dissipation is also increasing, which is challenging to accommodate using conventional cooling techniques. Therefore, this advancement of electronic components due to large-scale integration (LSI) on chips result in appliance with high power densities. This high-power density not only reduces the performance but also hinders the longevity of the electronic components. So, the thermal management is the main challenge to avoid the overheating such that through proper cooling technique the operating temperature can be maintained within the safer limit, the performance and life cycle of the component can be improved.

1.1. Types of electronics cooling

Impressive advancements have been made in cooling technology but are insufficient to meet today's cooling needs. The traditional and conventional techniques are falling short due to very low heat transfer coefficients (HTC). These techniques can be broadly classified into four categories based on their heat transfer mechanisms: radiation and free convection, forced air cooling, forced liquid cooling, and liquid evaporation. Liquid evaporation is the most efficient of these conventional techniques, whereas forced convection of air is the most widely used in cooling electronic components such as CPUs. Forced convection of air has a very low heat removing capacity; thus, using either Forced convection of liquid or Liquid evaporation is preferred.

1.2. Significance of heat sink

A heat sink is a passive heat exchanger that transfers the heat generated by an electronic device (chip) to a low temperature fluid medium. The main role of the heat sink is to maximize the surface area of contact between the hot surface and the surrounding cooling medium by using fins. The heat generated by the chip is transferred to the heat sink by conduction; subsequently, this heat is transferred to the surrounding, which is usually air, by convection

* Corresponding author.
E-mail address: deepakkumar.r@vit.ac.in (D. Rajagopal).

https://doi.org/10.1016/j.matpr.2022.09.251
2214-7853/
Selection and peer-review under responsibility of 2nd International Conference on Sustainable Materials, Manufacturing and Renewable Technologies 2022 (i-SMART 2022).

and radiation. Most often, heat spreaders are used between the chip and the heat sink due to the difference in size between the bottom of the sink and the top of the chip to ensure more heat dissipation. Heat sinks are attached to the surface of the spreader to provide additional surface area for heat removal by convection. The convection may be natural or forced air convection via a fan or duct. For high-power applications, it may be necessary to cool the chip directly with a heat pipe attachment, high-speed air jets, a direct heat sink attachment (cold plate), or dielectric liquid immersion. In electronic cooling, mini and microchannel heat sinks are prevalent in the industry due to the good efficiency of heat rejection on the small size of the said microchannels. The main challenge in designing a heat sink mechanism is optimizing the design to reduce the maximum operating temperature and minimum pressure drop.

2. Literature review

An extensive literature review was conducted to analyze the existing technology on pin-finned heat sinks with cross flow and jet impinging techniques and their applications in the electronics cooling industry. Boukhanouf and Haddad [1] conducted numerical experiments and reported that the operating temperature is reduced by increasing the copper base plate thickness and replacing the base plate with a vapor chamber. Based on computational fluid dynamics technique, Chu et al. [2] proposed a novel design of fin with triangular protrusions at the end of the fin, the predicted results also verified with experimental testing results. The results shows that the proposed design has less thermal resistance than conventional fins, the maximum temp is considerably reduced for the protrusion angle greater than 45°. Rashid et al. [3] studied the thermal characteristics of carbon nanotube based microchannels with varying fluid and flow conditions. A comparative study was conducted to analyze the maximum temperature rise, heat extraction and thermal stress on fins with different geometries and orientations. 1D and 2D arrays of fins were considered, along with a rectangular and circular cross-section of the fins. Different fluids (Water and glycol) were considered for the study. The results shows that the 2D circular pin fin was the most efficient with either of the working fluids. An alternate graphene-based working nanofluid was considered by Bahiraei et al.[4]. A comparative study between different nanofluid concentrations, fin geometry, and flow velocities has been conducted. The results include the variation of fin temperature, thermal resistance, temperature uniformity, convective coefficient, and pumping power. An increase in particle fraction of graphene and the flow velocity reduces the maximum operating temperature, increases temperature distribution, and reduces thermal resistance.

Freegah et al. [5] considered different fin geometries, including filleted and non-filleted fins, symmetrical semicircles, and corrugated semicircles on fins. The design was further optimized by reducing the pitch of the semicircle protrusions, and hollow semicircle protrusions were also studied. Plate-fin heat sinks with corrugated half-round pins in vertical arrangement subject to parallel flow were proved to be the most efficient configuration among all studied designs. Sarma et al. [6] conducted a comparative study between regular and splayed heat sinks with different materials and configurations. The results show lower splayed configuration temperatures than regular pin fins. The hybrid splayed configuration provide the most efficient way of cooling while the regular aluminum pin fins the least.

Different pin fin geometries such as zig-zag, fluted, slanted mirror, custom pin fin, and staggered were compared for their thermal efficiencies by Kulkarni and Dotihal [7]. The results show that the slanted mirror pin fins are the best configuration since they provide a high Nusselt number, low-pressure drop, and lower temperatures than other designs. [8] A comparative analysis of the thermal characteristics of hollow hybrid fins (HHF), solid hybrid fins (SHF), and regular pin fins and their orientations. Results indicate that the HHF and SHF show better thermal characteristics than regular pin fins. It is also concluded that the HHF performs better than the other two types. Li and Chen [9] investigated the effects of the fin width and the fin height of the heat sink on the heat transfer at different Reynolds numbers by numerical and experimental techniques. The thermal resistance decreases as the Reynolds number is increased. The optimized fin width of the heat sink depends on the Reynolds number, it increases with increasing Reynolds number. The thermal performance is improved as the fin height is increased initially, and further increase of the fin height reduces the performance of the heat sink. Chin et al. [10] studied the thermal characteristics of solid fins and perforate pin fins in convective heat transfer [10]. The pressure difference across the heat sink is more negligible with an increasing number of perforation and perforation diameter. The perforated pin fin array performs better than the solid pins in all cases. Nusselt number increases with an increasing number of perforation and perforation diameter.

3. Problem statement

Comparison between cross flow and jet impingement flow techniques are limited in literature, so an investigation is done to study the thermal characteristic of pin fins under different flow conditions. This study will provide a conclusive data comparing not only the conjugate heat transfer properties for either of the flows, but also the pumping power required to attain the results. A circular pin fin heat sink with 14 pin fins is considered for investigation. The diameter of the pin fin is taken to be 8 mm and its height is 50 mm. The length of the base plate is 95 mm, its thickness is 3 mm. The pin fins are placed 25 mm apart from each other. The 2D model of the pin fins is represented in Fig. 1.

3.1. Modelling of cross flow

The geometric model for the cross- flow technique consisted of a rectangular channel of length 1050 mm with a breadth and height of 100 mm and 50 mm respectively. The fins are placed 697.5 mm away from the inlet boundary, while the outlet is 257.5 mm downstream of the pin fins. The schematic is given in the Fig. 2. Velocity inlet and pressure outlet are considered as the boundary conditions.

3.2. Modelling of jet impingement

The domain for the jet impingement method is taken to be a box of dimensions 210x210x112 mm, where the pin fin is placed at the center of the computational domain. The orifice for the jet inlet is 65 mm above the pin fin and the orifice diameter is 13 mm. The 2D representation of the computational domain is shown in Fig. 3. Jet velocity is assigned at the center of the top surface of the computational domain and atmospheric pressure is imposed at all other boundaries.

4. Methodology

Computational fluid dynamics is used to solve the conjugate heat transfer problems associated with this research. In all the cases the pin fin employed is a circular pin fin with an array of 14 fins of 8 mm in diameter, 50 mm in length and are 25 mm apart from each other. SolidWorks tool is used to develop the three-

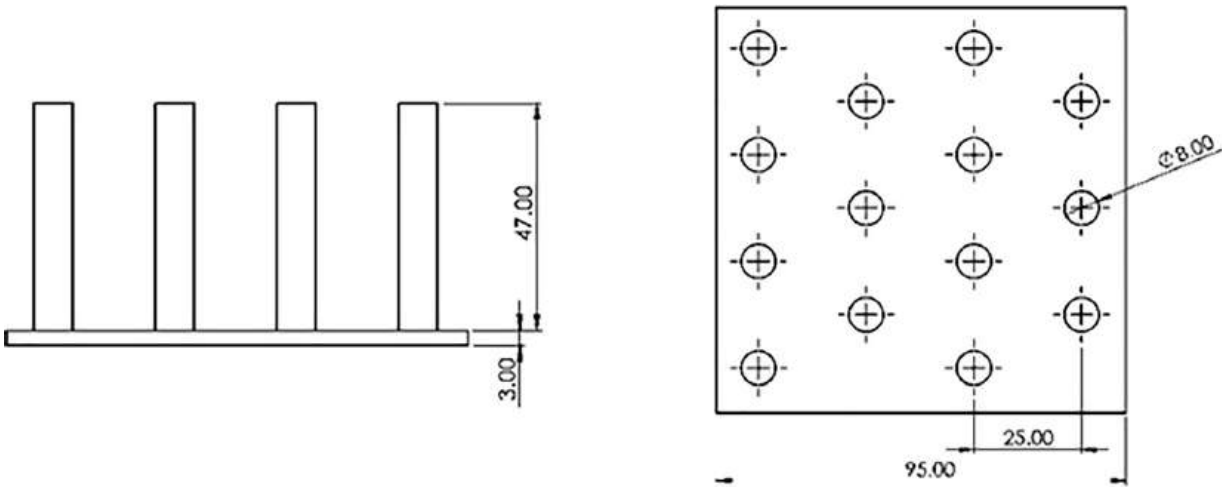

Fig. 1. 2D model of pin fins.

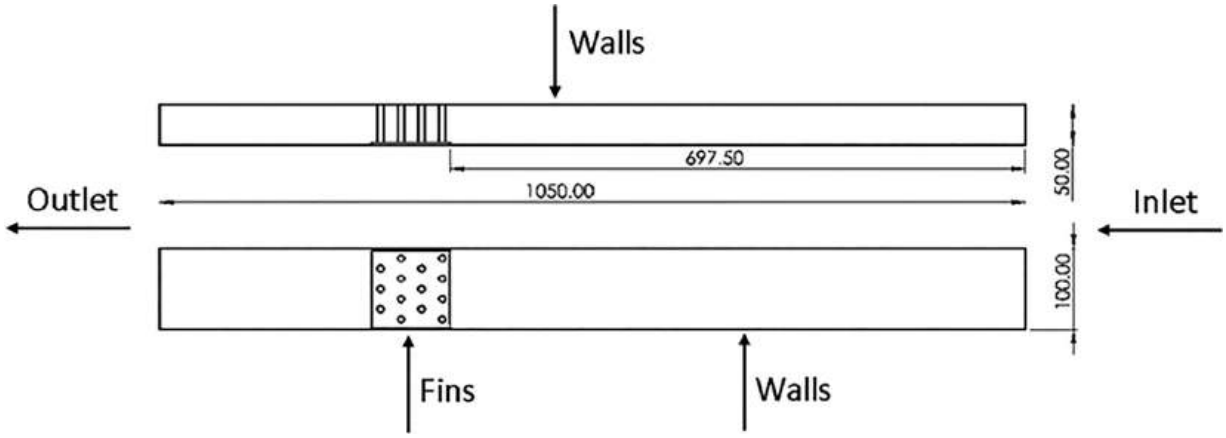

Fig. 2. Schematic of cross flow cooling.

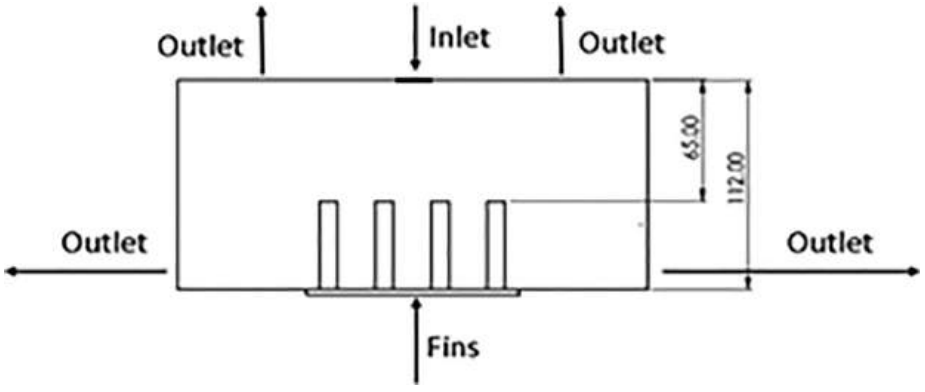

Fig. 3. Schematic of jet impingement cooling.

dimensional computational domain of the pin fins. The discretization of the domains is done using ICEM CFD, the quality of the mesh is ensure using grid sensitivity analysis, which is discussed in section 6.2. The schematic representation of mesh for the cross flow and jet impingement are shown in Fig. 4 and Fig. 5. The governing equations with appropriate boundary conditions mentioned in section 3.1 and 3.2 are solved using Ansys Fluent solver, due to its versatility.

The thermal energy generated by the electronic chip will be dissipated using convection, conduction and radiation. The radiation heat transfer is negligible due to the small difference in temperature between the pin fins and the ambient environment, it only amounts to 0.5 % of the total heat transfer[1]. The conduction heat losses amount up to 1.1 % of the total heat loss. Due to this convective heat transfer plays the major role in electronics cooling to dissipate all the residual heat.

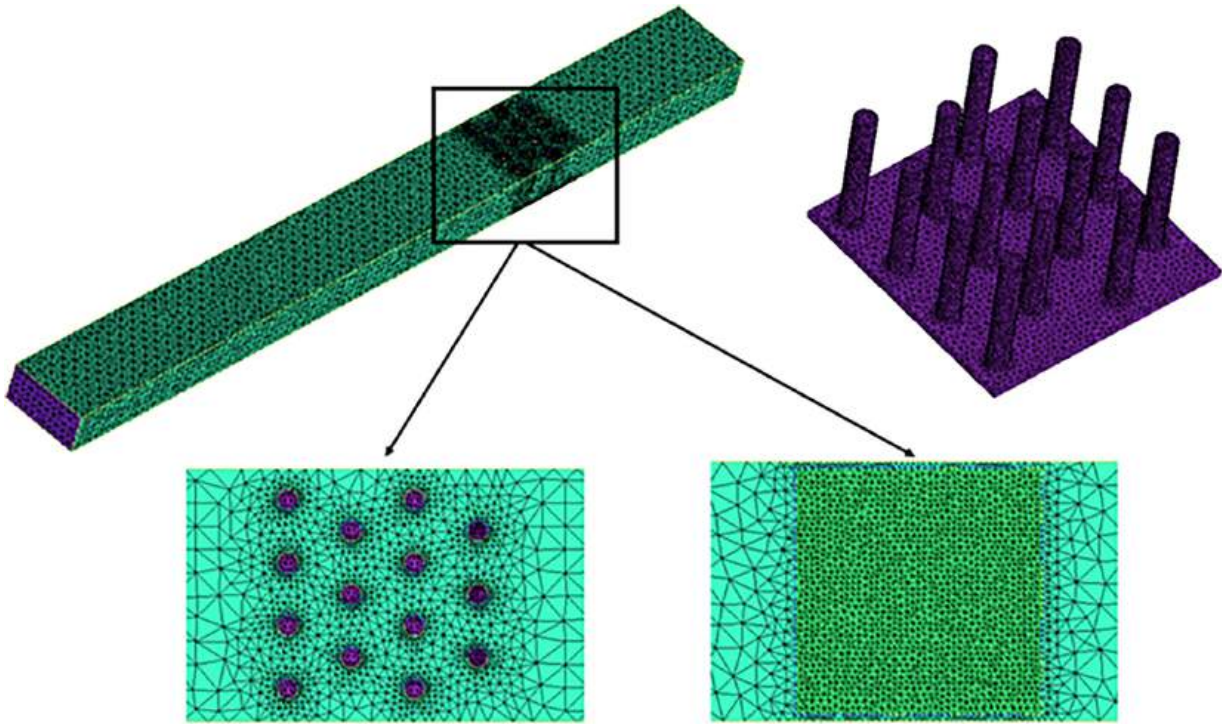

Fig. 4. Grid representation for cross flow domain.

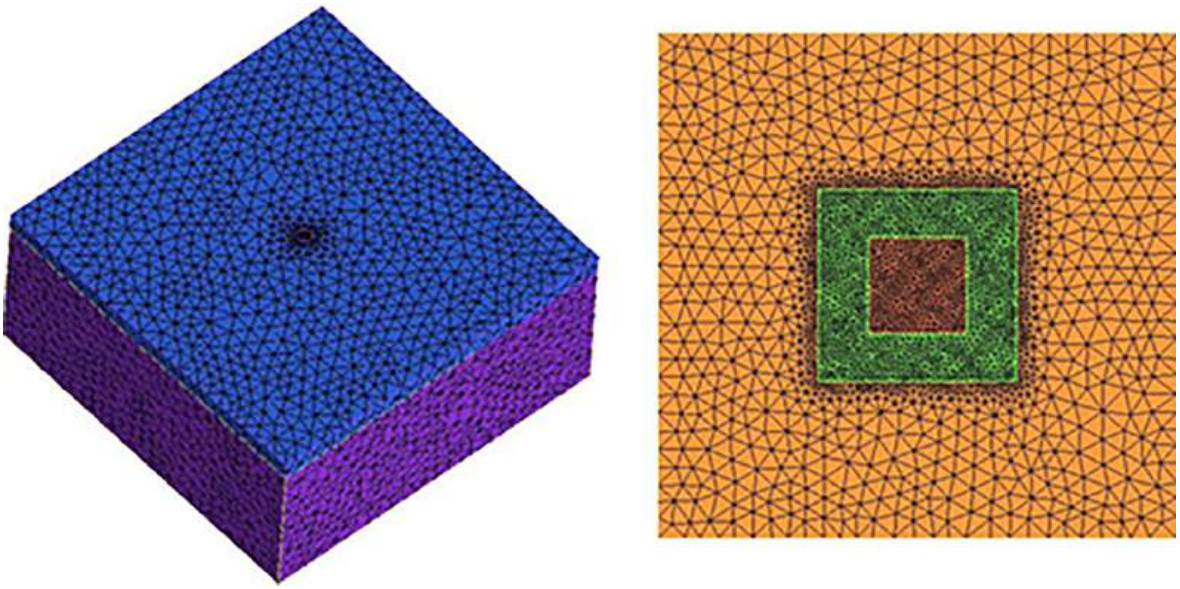

Fig. 5. Grid representation for jet impingement domain.

$$Q_{total} = Q_{conduction} + Q_{convection} + Q_{radiation} \quad (1)$$

The convective thermal energy that is dissipated can be represented by the equation.

$$q'' = \frac{0.984E}{A_b} \quad (2)$$

where, q'' is the convective thermal energy, E is the electrical power input due to which the heat is generated and A_b is the contact area of the fin. The convective heat transfer coefficient ($\bar{h}$), the Nusselt number ($\bar{Nu}$), pressure drop (ΔP), Reynolds number (Re) and the pumping power (P_p) are given by the following equations.

$$\bar{Nu} = \frac{q'' D_h}{k_{air}(T_w - \frac{T_{in}+T_{out}}{2})} \quad (3)$$

$$\bar{h} = \frac{\bar{Nu}\,.k_{air}}{D_h} \quad (4)$$

$$Re = \frac{\rho u_0 D_h}{\mu} \quad (5)$$

$$\Delta P = P_{in} - P_{out} \quad (6)$$

$$P_p = \Delta P.\dot{V} \tag{7}$$

The solid heat conduction equation is given by.

$$\frac{\partial}{\partial x}(\rho h) = \frac{\partial}{\partial x_i}\left(k\frac{\partial T}{\partial x_i}\right) + S_h \tag{8}$$

The hydraulic diameter for the jet impingement flow is taken to the orifice diameter i.e. 8 mm while that for the cross flow is calculated using the equation.

$$D_h = \frac{4A}{P_c} \tag{9}$$

The total area of heat transfer for the fins can be expressed as.

$$A_{fin} = WL + \pi Dn\left(H - \frac{D}{4}\right) \tag{10}$$

5. Turbulence modelling and boundary conditions

The finite volume-based solver Ansys Fluent is used to solve the steady state, incompressible flow, three dimensional Navier-Stokes and Energy equations. The realizable k-ϵ turbulence model with standard wall functions is used to predict the turbulence characteristics. SIMPLEC algorithm is used for coupling of velocity and pressure along with a second order discretization scheme. The convergence criteria were set to achieve 10^{-6} for the scaled residuals. The flow has been simulated with respect to Reynolds number. The characteristic length for the cross flow is considered to be the cross section of the rectangular flow channel, while that of the jet impingement technique is taken to be the orifice diameter of the inlet.

The governing equations are summarized as follows:

Continuity equation

$$\nabla.\left(p\vec{v}\right) = 0 \tag{11}$$

Momentum equation

$$\rho\vec{v}.\nabla\vec{v} = \mu\nabla^2\vec{v} - \nabla P \tag{12}$$

Energy equation

$$\rho c_p\nabla.\left(\vec{v}T\right) = \nabla.(k\nabla T) \tag{13}$$

k-ϵ realisable transport equations

$$\frac{\partial}{\partial x_j}(\rho\kappa u_j) = \frac{\partial}{\partial x_j}\left[\left(\mu + \frac{\mu_t}{\sigma_k}\right)\frac{\partial\kappa}{\partial x_j}\right] + G_\kappa + G_b + \rho_\epsilon + Y_M \tag{14}$$

$$\frac{\partial}{\partial x_j}(\rho\epsilon u_j) = \frac{\partial}{\partial x_j}\left[\left(\mu + \frac{\mu_t}{\sigma_k}\right)\frac{\partial\epsilon}{\partial x_j}\right] - \rho C_2\frac{\epsilon^2}{\kappa + \sqrt{\vartheta\epsilon}} + C_{1\epsilon}\frac{\epsilon}{\kappa}C_{3\epsilon}G_b \tag{15}$$

5.1. Numerical setup for cross flow cooling

A heat flux of 5903 W/m^2 is given at the base of the pin fin. No slip wall boundary conditions are given to the pin fin walls and the channel walls. The hydraulic diameter is taken as 0.067 m and the turbulence intensity is taken as 10 %. All the other walls are considered to be adiabatic except the base of the fins. The Reynolds number for the cross-flow technique is given by.

$$Re = \frac{\rho u_0 D_h}{\mu} \tag{16}$$

Where,

$$D_h = \frac{4A}{P_c} \tag{17}$$

5.2. Numerical setup for jet impingement cooling

The heat flux given in this case is same as the cross-flow setup which is 5903 W/m2 at the base of the pin fin. The inlet is given at the orifice at the top of the domain whilst all the other faces are considered as pressure outlets. The base of the domain is considered as adiabatic wall. The governing equations for this setup are same as above. The Reynolds number calculations for jet impingement cooling can be calculated using the equation (18). Where, D is the diameter of the orifice, which is taken as 8 mm.

$$Re = \frac{\rho VD}{\mu} \tag{18}$$

6. Results and discussion

This section compares the thermal characteristics of pin fin heat sinks in cross flow and jet impingement flow techniques. First, the CFD model is validated with respect to the existing experimental and numerical results published from the past literature. Then, similar models are simulated using CFD for cross flow and jet impingement with varying Reynold's number.

6.1. Validation results

Validation of the present computational methodology has been ensured with previous studies on the basis of two literature papers respectively for cross flow and jet impingement of cooling.

6.1.1. Validation of cross flow heat sink

The aim of this validation is to ensure the computational method, which leads to increase the confident level on the accuracy of numerical results for further parametric investigations. The cross-flow model is validated with respect to the existing experimental results of Li and Chen [9], the maximum deviation of predicted results from the literature is 1.5 %. Fig. 6 (a) shows the comparison of Nusselt number with respect to increasing Reynolds number.

6.1.2. Validation of jet impingement heat sink

In case of jet impingement model, the computational methodology is validated with the results of Jeng *et al.* [13]. The variation of predicted Nusselt number with respect to Reynolds number is compared with the existing literature results, it is represented in Fig. 6 (b). The maximum difference of Nusselt number between the predicted and the literature results is 1.9 %.

6.2. Grid independence study

In grid sensitivity analysis, it is preferred to monitor the parameter in a nodal point of the computational domain instead of averaged quantity with respect to various set of grid size [14–17]. But in this study, considering the base temperature of heat sink at the center will be in appropriate due to two different flow approaching the heat sink, so the surface averaged base temperature is taken as a study parameter for grid sensitivity analysis. a three-dimensional discretized model is created using the tool ICEM CFD in the pre-processor phase. Since the type and the quality of the girds heavily influence the results, the domain is discretized as tetrahedral unstructured mesh due to formation of complex geometry in the interface of pin fin and base. The details and comparison of the grids and the results are given in Fig. 6 (c). The finest grid chosen was 0.7 million grids while the coarse mesh was 0.06 million grids. The error for 0.06 million cells is 3.8 % while that of other sizes is less than one. Based on better numerical accuracy and less compu-

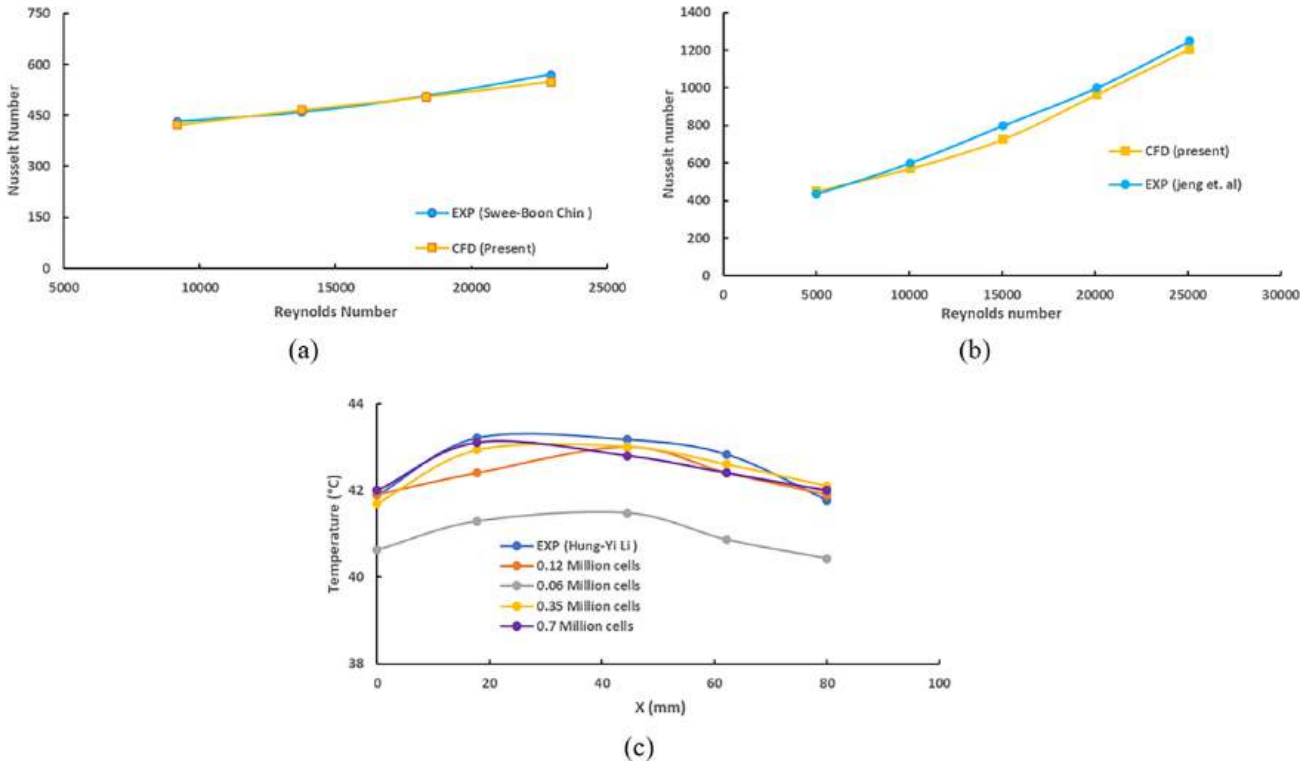

Fig. 6. Results of (a) Validation (cross flow) (b) Validation (jet impingement) (c) Grid independence.

tation time, the grid size of 0.12 million is taken as an optimum grid size.

6.3. Comparison of cross flow and jet impingement cooling

As this present work is focused to compare the thermal characteristics of pin fin heat sink under different flow conditions, the variation of Nusselt number with respect to Reynolds number is plotted and compared for both cross flow as well as jet impingement. The Fig. 7 (a) shows the variation of Nusselt number for the Reynolds number varying from 9000 to 32000. The increasing trend of Nusselt number is similar for both the cases, but the Nusselt number of cross-flow conditions is significantly higher than the jet impingement for a particular Reynolds number. The Nusselt number is compared for cross flow with respect to [11]. It is observed that the Nusselt number obtained from our setup is higher by two folds comparatively. This is due to the greater available contact surface area for convection because of higher fin height in the present model. To further understand the heat transfer characteristics, Nusselt number from [12] is considered, it is observed that even for higher fin density, the Nusselt number is significantly low due to lower fluid velocity. The Nusselt number of square pin fins of 5x5 grid are compared for jet impingement technique from the experimental data [13]. It is noted that the square pin fins with in-line configuration show better thermal characteristics for a fixed Reynolds number than the present model. This is due to the greater size of the square fins, which enables better convective heat transfer properties.

Further, the base temperature of heat sink is compared in Fig. 7 (b), it decreases with increasing Reynolds number, the jet impinged heat sink has higher base temperature as compared to the cross-flow technique for all the Reynolds number studied. It is also ensured from temperature contour shown in Fig. 8(a) and 8(b) respectively for cross flow and jet impingement. In particular, at lower Reynolds number, the base temperature of jet impinging techniques is very high as compared to cross flow. But the significance becomes lesser at higher Reynolds number. This is due to the heat transfer in jet impinging technique is focused at the centre of heat sink base striking by a small jet, whereas in cross flow the heat interaction occurs from one leading edge of the heat sink. But at higher Reynolds number, more amount of air is contacted at the base centre from where the heat is propagating, thus the deviation between cross flow and jet impinging technique becomes lesser as compared with low Reynolds number. The comparison of pumping power is shown in Fig. 7(c), the pumping power increases with respect to increasing Reynolds number. The pumping power of jet impingement method is more as compared to the cross flow, since the jet impingement requires higher pressure of air at the inlet to produce a high velocity jet. The variation of pressure drop across the heat sink is compared for both the flows which is shown in Fig. 7(d). The pressure drop increase with increasing Reynolds number in both the cases, but the magnitude of increase is much higher in the jet impingement technique. Also, the pressure drop for cross flow is significantly less than that of jet impingement for all the studied Reynolds number. As mentioned earlier, the increasing pressure drop is attributed to high pressure jet at the inlet. From these results it is understand that cross flow technique produces efficient cooling than the jet impingement technique.

7. Conclusion

A comparative analysis has been carried out between cross flow and jet impingement cooling methods to analyze the thermal characteristics of pin fins. The major findings are listed below.

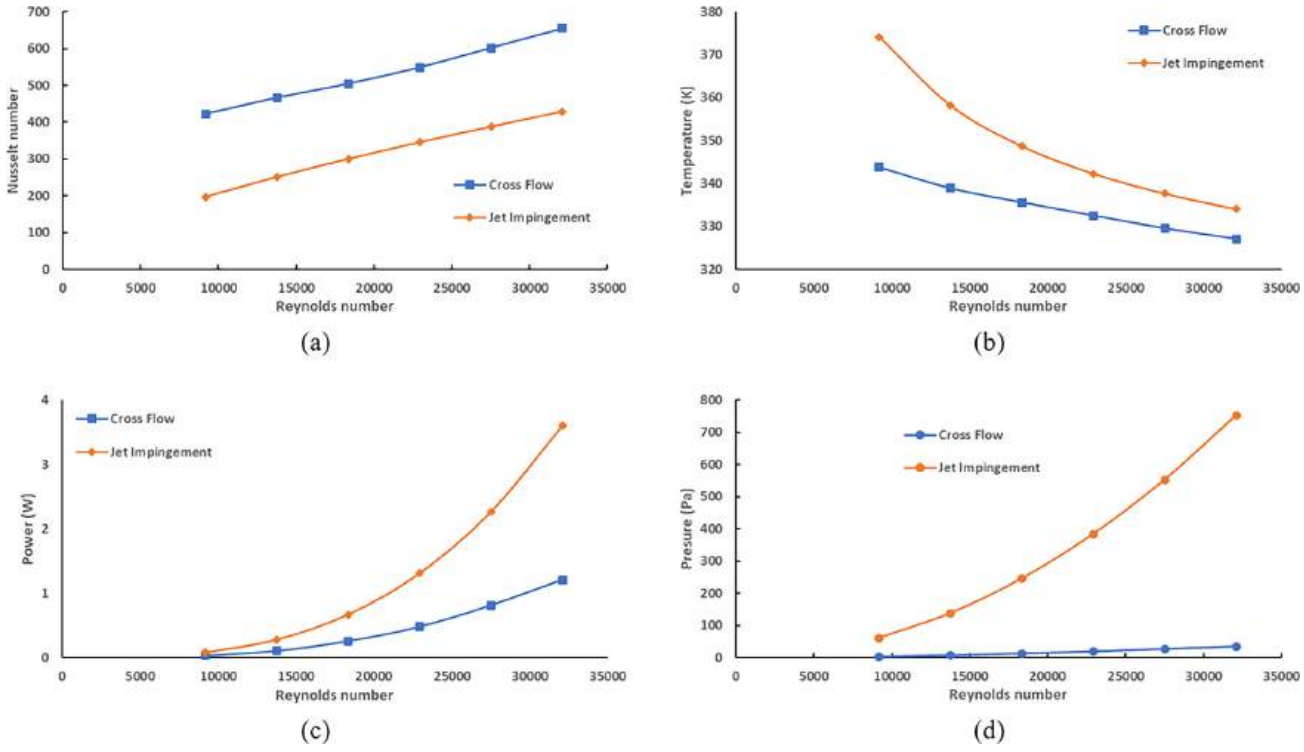

Fig. 7. Comparison of (a)Base temperature (b)Pumping power (c)Pressure drop (d)Thermal resistance.

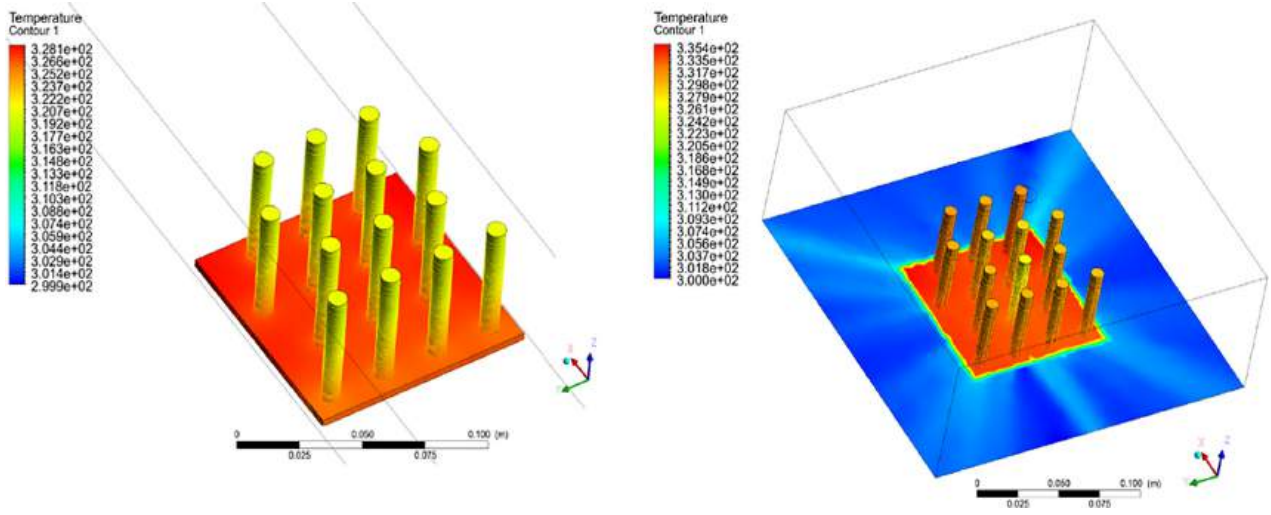

Fig. 8. Temperature contour of pin fin in (a) cross flow (b) jet impingement.

- The Nusselt number increases with the increase in Reynolds number for both cases. The difference between the two techniques remains same throughout Reynold's number studied. The cross-flow yield a higher Nusselt number than the jet impingement flow, with an average difference of 41.1 %.
- A lower pressure drop is favorable since it consumes less power. But it is observed that the pressure drop among the two techniques is low at low Reynolds number, whereas it increases significantly for the jet impingement case at higher Reynolds number.
- It is noticed that the jet impingement flow demands a higher pumping power to achieve the same results as the cross flow produces. As a result, the jet impingement flow requires an average of 61 % of more pumping power for the same configuration. The base temperature under steady-state conditions is noticeably lower in the case of cross-flow with an average reduction of 14.5° C.
- It is concluded that the cross-flow has better thermal characteristics as compared to the jet impingement technique in all the Reynolds number studied, particularly the significant is more at lower Reynolds number. Even though the cooling in cross flow technique is better at a higher Reynolds number, the trend shows that the further increase in Reynolds number may have significant effect in jet impingement cooling than the cross-flow technique. Overall, the thermal performance of the cross-flow technique is superior than the jet impingement technique, with respect to higher in Nusselt number, lower in base temperature, pressure drop and pumping power.

CRediT authorship contribution statement

Deerajkumar Parthipan: Writing – original draft, Methodology, Software, Formal analysis, Investigation, Validation, Visualization. **R. Deepakkumar:** Conceptualization, Project administration, Supervision, Data Curation, Writing – review & editing.

Data availability

Data will be made available on request.

Declaration of Competing Interest

The authors declare that they have no known competing financial interests or personal relationships that could have appeared to influence the work reported in this paper.

Acknowledgements

Authors wish to thank the Computational Fluid Dynamics (CFD) laboratory, Department of Thermal and Energy Engineering, SMEC, Vellore Institute of Technology, Vellore for the support to conduct this research work successfully.

References

[1] R. Boukhanouf, A. Haddad, A CFD analysis of an electronics cooling enclosure for application in telecommunication systems, Appl. Therm. Eng. 30 (16) (2010) 2426–2434, https://doi.org/10.1016/j.applthermaleng.2010.06.012.
[2] W.-X. Chu, M.-K. Tsai, S.-Y. Jan, H.-H. Huang, C.-C. Wang, CFD analysis and experimental verification on a new type of air-cooled heat sink for reducing maximum junction temperature, Int. J. Heat Mass Transf. 148 (2020) 119094.
[3] M.A.I. Rashid, M.F. Ismail, M. Mahbub, CFD Analysis in a Liquid-Cooled Carbon Nanotube Based Micro-channel Heatsink for Electronic Cooling, Int. J. Eng. Technol. 3 (5) (2011) 553–559, https://doi.org/10.7763/IJET.2011.V3.284.
[4] M. Bahiraei, S. Heshmatian, M. Goodarzi, H. Moayedi, CFD analysis of employing a novel ecofriendly nanofluid in a miniature pin fin heat sink for cooling of electronic components: Effect of different configurations, Adv. Powder Technol. 30 (11) (2019) 2503–2516, https://doi.org/10.1016/j.apt.2019.07.029.
[5] B. Freegah, A.A. Hussain, A.H. Falih, H. Towsyfyan, CFD analysis of heat transfer enhancement in plate-fin heat sinks with fillet profile: Investigation of new designs, Therm. Sci. Eng. Prog. 17 (2020) 100458.
[6] A. Sarma, A. Ramakrishna, P.G. Student, CFD Analysis of Splayed Pin Fin Heat Sink for Electronic Cooling, Int. J. Eng. Res. Technol. 1 (10) (2012).
[7] V.M. Kulkarni, B. Dotihal, CFD and conjugate heat transfer analysis of heat sinks with different fin geometries subjected to forced convection used in electronics cooling, Int. J. Res. Eng. Technol. 4 (6) (2015).
[8] Kyoung Joon Kim, Orientation effects on the performance of natural convection cooled hybrid fins, in: 20th International Workshop on Thermal Investigations of ICs and Systems, 24–26 Sept. 2014. https://doi.org/10.1109/Therminic34607.2014.
[9] H.-Y. Li, K.-Y. Chen, Thermal-Fluid Characteristics of Pin-Fin Heat Sinks Cooled by Impinging Jet, J. Enh. Heat Transf. 12 (2) (2005) 189–202.
[10] S.B. Chin, J.J. Foo, Y.L. Lai, T.K.K. Yong, Forced convective heat transfer enhancement with perforated pin fins, Heat Mass Transf. 49 (10) (2013) 1447–1458, https://doi.org/10.1007/s00231-013-1186-z.
[11] F. Zhou, I. Catton, Numerical evaluation of flow and heat transfer in plate-pin fin heat sinks with various pin cross-sections, Numer. Heat Transf. A Appl. 60 (2) (2011) 107–128, https://doi.org/10.1080/10407782.2011.588574.
[12] J. Zhao, S. Huang, L. Gong, Z. Huang, Numerical study and optimizing on micro square pin-fin heat sink for electronic cooling, Appl. Therm. Eng. 93 (2016) 1347–1359, https://doi.org/10.1016/j.applthermaleng.2015.08.105.
[13] T.M. Jeng, S.C. Tzeng, H.R. Liao, Flow visualizations and heat transfer measurements for a rotating pin-fin heat sink with a circular impinging jet, Int. J. Heat Mass Transf. 52 (7–8) (2009) 2119–2131, https://doi.org/10.1016/j.ijheatmasstransfer.2008.10.028.
[14] R. Deepakkumar, S. Jayavel, Effect of local waviness in confining walls and its amplitude on vortex shedding control of the flow past a circular cylinder, Ocean Eng. 156 (2018) 208–216, https://doi.org/10.1016/j.oceaneng.2018.03.018.
[15] R. Deepakkumar, S. Jayavel, S. Tiwari, A comparative study on effect of plain and wavy-wall confinement on wake characteristics of flow past circular cylinder, Sadhana 42 (6) (2017) 963–980, https://doi.org/10.1007/s12046-017-0649-1.
[16] R. Deepakkumar, S. Jayavel, S. Tiwari, Cross flow past circular cylinder with waviness in confining walls near the cylinder, J. Appl. Fluid Mech. 10 (1) (2017) 183–197, https://doi.org/10.18869/acadpub.jafm.73.238.26148.
[17] R. Deepakkumar, S. Jayavel, S. Tiwari, Computational study of fluid flow characteristics past circular cylinder due to confining walls with local waviness, J. Phys. Conf. Series 759 (2016), https://doi.org/10.1088/1742-6596/759/1/012083 012083.